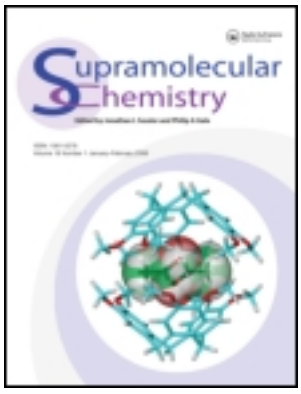

Supramolecular Chemistry
Publication details, including instructions for authors and subscription information:
http://www.tandfonline.com/loi/gsch20

Synthesis, characterisation and electrochemistry of derivatisable novel α-tetra 7-oxycoumarin-3-carboxylate-substituted metallophthalocyanines

Eyüp Dur [a], Ali Rıza Özkaya [a] & Mustafa Bulut [a]
[a] Department of Chemistry, Marmara University, 34722, Göztepe, Istanbul, Turkey

Available online: 13 Apr 2011

To cite this article: Eyüp Dur, Ali Rıza Özkaya & Mustafa Bulut (2011): Synthesis, characterisation and electrochemistry of derivatisable novel α-tetra 7-oxycoumarin-3-carboxylate-substituted metallophthalocyanines, Supramolecular Chemistry, 23:05, 379-388

To link to this article: http://dx.doi.org/10.1080/10610278.2010.521829

Supramolecular Chemistry
Vol. 23, No. 5, May 2011, 379–388

Taylor & Francis
Taylor & Francis Group

Synthesis, characterisation and electrochemistry of derivatisable novel α-tetra 7-oxycoumarin-3-carboxylate-substituted metallophthalocyanines

Eyüp Dur, Ali Rıza Özkaya* and Mustafa Bulut*

Department of Chemistry, Marmara University, 34722 Göztepe, Istanbul, Turkey

(*Received 23 April 2010; final version received 29 August 2010*)

Novel α-tetra-substituted metallophthalocyanines (ZnPc (**3**), CoPc (**4**), CuPc (**5**) and NiPc (**6**)) have been synthesised by cyclotetramerisation of a novel ligand, ethyl 7-(2,3-dicyanophenoxy)coumarin-3-carboxylate, with the relevant metal acetates. In addition, two derivatives of **3**, slightly water-soluble tetrakis[7-oxycoumarin-3-carboxylic acid] phthalocyaninatozinc(II) and tetrakis[7-oxo-3-(ethyl piperidine-3-carboxlate)-coumarin]phthalocyaninatozinc(II), were prepared by its reaction with HCl (37%) and heating with ethyl 3-piperidinecarboxylate, respectively. The newly prepared compounds have been characterised by FT-IR, UV–vis, MALDI-TOF mass and ^{1}H NMR spectroscopies. The redox behaviour of **3**–**6** was also investigated by voltammetry and *in situ* spectroelectrochemistry.

Keywords: metallophthalocyanine; coumarin; alpha substitution; ethyl nipecotate; electrochemistry

Introduction

Metallophthalocyanines (MPcs) are full-aromatic 18π-electron heterocyclic conjugated compounds that have been a focus of attention because of their exclusive properties. These compounds have been attracting great technological and commercial interest not only as dyes, but also as conductive, catalytic, photocatalytic and electrochromic advanced materials. Some other applications of MPcs have also appeared, such as photodynamic therapy (PDT), gas sensors, solar cell technology, optical read–write discs and nonlinear optics (*1*, *2*).

A major disadvantage of Pcs and MPcs is their low solubility in organic solvents or water. It has been found that suitable functional groups such as carboxyl, sulphonyl and quaternised ammonium groups in the periphery or non-periphery of the Pc ring can improve the solubility in protic or aprotic solvents (*3*). Thus, the synthesis of the functional/reactive Pcs has become an interesting target for chemists (*4*). The involvement of four coumarin entities in the periphery of the Pc ring after the cleavage of all four lactone rings was found to increase its solubility (*5*). On the other hand, coumarins (2H-chromen-2-ones) belong to a very large class of oxygen heterocycles found in nature (*6*). Compounds containing a coumarin moiety display a broad spectrum of biological activities such as antifungal (*7*), anticoagulant, vasodilator, estrogenic, dermal, photosensitising, sedative, hypnotic, analgesic, antimicrobial (*8*), anti-inflammatory, anti-HIV (*9*) and antiulcer activities (*10*). Coumarin and 7-hydroxycoumarins exhibit cytotoxic effects against the lung adenocarcinoma cell lines KB (*11*). Some coumarins show anti-clotting activity (*12*). For example, carbochromene (3-diethylaminoethyl-7-ethoxycarbonyl-methoxy-4-methylcoumarin) is a potent specific coronary vasodilator, used for many years in the treatment of angina pectoris (*13*). Moreover, coumarins are widely used as additives in food and cosmetics (*14*), dispersed fluorescent, laser dyes and optically brightening agents (*15*). They can also be used as functional peripheral or non-peripheral groups for the synthesis of novel useful Pcs (*4*, *16*, *17*). Within the class of 7-hydroxycoumarins that typically display favourable fluorescence and lasing properties, the derivatives that bear additional carboxylate substituents at the 3-position have several differentiating properties. Attachment of a lipophilic moiety to the nitrogen atom of the nipecotic acid leads to a compound that readily cross the blood–brain barrier. This type of compounds acts as inhibitory neurotransmitter in mammalian central nervous system. Therefore, they can be used for the treatment of pain, anxiety and epilepsy (*18*, *19*). 7-Hydroxycoumarins allow the binding of this structure to a Pc via a phenoxy bond (*20*). This covalent binding should not significantly affect the biological activity of the coumarin moiety. The combination of coumarin and Pc may produce candidate molecules for PDT applications (*21*). In view of the biological importance of both ethyl 7-hydroxycoumarin-3-carboxylate and Pcs, it is worthwhile to combine these two functional molecules into a single compound via synthetic methodology and to prepare and characterise their soluble MPcs, which may also exhibit biological activities.

This study concerns the synthesis, characterisation and structural investigation of α-tetra (ethyl 7-oxycoumarin-3-carboxylate)-substituted Zn(II), Co(II), Cu(II) and Ni(II)

*Corresponding authors. Email: aliozkaya@marmara.edu.tr; mbulut@marmara.edu.tr

ISSN 1061-0278 print/ISSN 1029-0478 online

DOI: 10.1080/10610278.2010.521829
http://www.informaworld.com

Pcs (**3**–**6**). In addition, the ethyl carboxylate functional groups of coumarino-ZnPc (**3**) were hydrolysed with 37% aqueous hydrochloric acid in *N*,*N*-dimethylformamide (DMF) at 120°C to prepare water-soluble coumarino-ZnPc carrying a carboxylic acid group in position 3 of each coumarin (**3a**). The ZnPc (**3**) was reacted with ethyl nipecotate to demonstrate the derivatisability of ZnPc (**3**). The ligand (**1**) and the complexes (**3**–**6**, **3a** and **3d**) were characterised using physico-chemical methods such as ^{1}H NMR spectra, elemental analysis, mass, electronic and IR spectral measurements. The novel MPcs (**3**–**6**, **3a** and **3b**) displayed good solubility in common organic solvents such as tetrahydrofuran (THF), DMF, dimethylacetamide (DMA) and dimethylsulphoxide (DMSO).

Experimental

Synthesis

Ethyl 7-hydroxycoumarin-3-carboxylate and the starting material, 1,2-dicyano-3-nitrobenzene, were prepared by the reported procedures (*16*, *17*). The purities of ethyl 7-hydroxycoumarin-3-carboxylate and 1,2-dicyano-3-nitrobenzene were tested in each step by TLC. Routine IR spectra were recorded on a Shimadzu Fourier Transform FTIR-8300 infrared spectrophotometer using KBr pellets. The electronic spectra were monitored on a Shimadzu UV-2450 UV–vis spectrophotometer. ^{1}H NMR spectra were recorded on a Varian Unity Inova 500 MHz NMR spectrophotometer using TMS as the internal reference at Gebze Institute of Technology. Elemental analysis was performed by the Instrumental Analysis Laboratory of TUBITAK Ankara Test and Analysis Laboratory. Mass spectra were performed on a Bruker Daltonic Autoflex III MALDI-TOF spectrometer at Marmara University.

*Synthesis of ethyl 7-(2,3-dicyanophenoxy) coumarin-3-carboxylate (**1**)*

Ethyl 7-hydroxycoumarin-3-carboxylate (1.00 g, 4.27 m mol) and 1,2-dicyano-3-nitrobenzene (0.74 g, 4.27 mmol) were dissolved in dry DMF (100 ml), and anhydrous K_2CO_3 (0.89 g, 6.41 mmol) was added and the mixture was heated and stirred for 24 h under nitrogen at 50–60°C. The reaction mixture was treated with diluted HCl under ice cooling. The brown precipitate was filtered, washed with water to neutralise and dried. It was soluble in THF, $CHCl_3$, DMF, DMA and DMSO. Yield: 0.89 g (58%); mp 236–239°C. FT-IR (KBr) ν_{max} (cm^{-1}): 3051–2997 (Ar-H), 2939–2918 (aliphatic CH), 2232 (C ≡ N), 1737 (C═O), 1571–1491 (Ar C═C), 1249 (Ar-O-Ar), 1142, 1102, 1037, 1006, 871, 843, 797, 731, 633, 551, 536, 454. ^{1}H NMR (DMSO-d_6) δ (ppm): 8.81 (s, 1H), 8.04 (br d, J = 8.5 Hz, 1H), 8.00 (br d, J = 8.5 Hz, 1H), 7.92 (br t, J = 8.5 Hz, 1H), 7.61 (d, J = 8.5 Hz, 1H), 7.33 (s, 1H), 7.27 (br d, J = 8.5 Hz, 1H), 4.30 (q, J = 7 Hz, 2H), 1.32 (t, J = 7 Hz, 3H). MS (MALDI-TOF) *m/z*: 396 [M]$^+$ + 2H$_2$O. UV–vis λ_{max} (nm) (log ε) in DMF: 314 (4.37).

*General procedure for the synthesis of 1(4),8(11),15(18), 22(25)-tetrakis[ethyl 7-oxycoumarin-3-carboxylate] phthalocyaninatometal derivatives (**3**–**6**)*

A mixture of compound **1** (0.1 g, 0.27 mmol) and 0.025 mmol metal salts [$Zn(OAc)_2{\cdot}2H_2O$ 0.014 g, $Co(OAc)_2{\cdot}4H_2O$ 0.016 g, Cu(OAc) 0.009 g, $Ni(OAc)_2{\cdot}4H_2O$ 0.016 g] in 2-chloronaphthalene (2 ml) was heated and stirred at 170°C for 24 h under N_2 in a sealed glass tube. After cooling to room temperature, the resulting green-blue mixture was precipitated by ethanol and filtered off. The product was washed with water, hot ethanol, acetone, diethylether and then dried.

*Synthesis of 1(4),8(11),15(18),22(25)-tetrakis[ethyl 7-oxycoumarin-3-carboxylate]phthalocyaninatozinc(II) (**3**)*

The compound was soluble in THF, DMF, DMA, DMSO. Yield: 0.036 g (36%). Mp > 300°C. FT-IR (KBr) ^{1}H NMR (DMSO). FT-IR (KBr) ν_{max} (cm^{-1}): 3073–3048 (Ar-H), 2981–2867 (aliphatic CH), 1728 (C═O), 1606–1477 (Ar C═C), 1333–1233 (Ar-O-C), 1116, 995, 812, 745, 616. UV–vis λ_{max} (nm) (log ε) in DMF: 317 (4.55), 618 (3.96), 688 (4.69). (MALDI-TOF, α-CHCA as matrix) *m/z*: 1507.61 [M + H]$^+$. Anal. Calcd for $C_{80}H_{48}N_8O_{20}Zn$: C, 63.71; H, 3.18; N, 7.43; O, 21.24%. Found: C, 63.74; H, 3.21; N, 7.34; O, 21.25%.

*Synthesis of 1(4),8(11),15(18),22(25)-tetrakis [7-oxycoumarin-3-carboxylic acid] phthalocyaninatozinc(II) (**3a**)*

A solution of 1(4),8(11),15(18),22(25)-tetrakis[ethyl 7-oxy coumarin-3-carboxylate]phthalocyaninatozinc(II) (**3**) (0.030 g, 0.019 mmol) in DMF (4 ml) containing water (1.42 ml) and concentrated hydrochloric acid (37%, 0.14 ml) was refluxed for 12 h. After cooling to room temperature, the resulting mixture was precipitated by ice and collected by centrifuge. Then, the product was washed with water to neutralise and dried in a vacuum oven. It was soluble in $CHCl_3$ (chloroform), THF, DMF, DMA and DMSO. Yield: 0.020 g (72%). Mp > 300°C. FT-IR (KBr) ν_{max} (cm^{-1}): 3374–3141 (carboxyl OH), 1714 (lactone, —C═O), 1652–1402 (Ar, —C═C—), 1339–1219 (Ar-O-C), 1049, 951, 795, 740. UV–vis λ_{max} (nm) (log ε) in DMF: 313 (4.68), 613 (4.19), 684 (4.96). (MALDI-TOF, α-CHCA as matrix) *m/z*: 1394 [M]$^+$. Anal. Calcd for $C_{72}H_{32}N_8O_{20}Zn$: C, 61.95; H, 2.31; N, 8.04; O, 22.95%. Found: C, 61.78; H, 2.34; N, 8.11; O, 22.46%.

*Synthesis of 1(4),8(11),15(18),22(25)-tetrakis [7-oxo-3-(ethyl piperidine-3-carboxlate)-coumarin]phthalocyaninatozinc(II) (**3b**)*

Potassium *tert*-butoxide (2.2 mg, 0.02 mmol) was added to a premixed mixture of ethyl nipecotate (3.1 mg, 0.02 mmol) and 1(4),8(11),15(18),22(25)-tetrakis[ethyl 7-oxycoumarin-3-carboxylate]phthalocyaninatozinc(II) (**3**) (0.030 g, 0.02 mmol). Then, the mixture was heated and stirred at 100°C for 24 h in a sealed glass tube. On completion of the reaction, the mixture was extracted with $CHCl_3$. After the evaporation of the solvent and purification, the light green product (**3b**) was obtained. It was soluble in $CHCl_3$, THF, DMF, DMA and DMSO. Yield: 0.022 g (56%). Mp > 300°C. FT-IR (KBr) ν_{max} (cm^{-1}): 3098–3021 (Ar-H), 2961–2858 (aliphatic CH), 1724 (—C═O), 1630–1439 (Ar, —C═C—), 1375–1258 (Ar-O-C), 1175, 1090, 1014, 856, 703. UV–vis λ_{max} (nm) (log ε) in DMF: 308 (4.40), 700 (4.33). (MALDI-TOF, α-CHCA as matrix) *m/z*: 1951 $[M]^+$. Anal. Calcd for $C_{88}H_{60}N_{12}O_{20}Zn$: C, 64.02; H, 4.34; N, 8.61; O, 19. 68%. Found: C, 64.76; H, 4.45; N, 8.66; O, 19.79%.

*Synthesis of 1(4),8(11),15(18),22(25)-tetrakis [ethyl 7-oxycoumarin-3-carboxylate] phthalocyaninatocobalt(II) (**4**)*

The compound was soluble in THF, DMF, DMA and DMSO. Yield: 0.031 g (32%). Mp >300°C. FT-IR (KBr) ν_{max} (cm^{-1}): 3071–3056 (Ar-H), 2930–2850 (aliphatic CH), 1710 (C═O), 1586–1475 (Ar C═C), 1329–1236 (Ar-O-C), 1119, 996, 801, 747. UV–vis λ_{max} (nm) (log ε) in DMF: 302 (4.96), 615 (3.86), 689 (4.56). (MALDI-TOF, α-CHCA as matrix) *m/z*: 1501.21 $[M + H]^+$. Anal. Calcd for $C_{80}H_{48}N_8O_{20}Co$: C, 64.05; H, 3.22; N, 7.47; O, 21.33. Found: C, 64.11; H, 3.27; N, 7.23; O, 21.51%.

*Synthesis of 1(4),8(11),15(18),22(25)-tetrakis [ethyl 7-oxycoumarin-3-carboxylate] phthalocyaninatocopper(II) (**5**)*

The compound was soluble in DMF, DMSO and DMA. Yield: 0.023 g (22%). Mp >300°C. FT-IR (KBr) ν_{max} (cm^{-1}): 3075–3030 (Ar-H), 2924–2851 (aliphatic CH), 1718 (C═O), 1610–1458 (Ar C═C), 1325–1258 (Ar-O-C), 1122, 1001, 802, 746, 618. MS (MALDI-TOF, α-CHCA as matrix) *m/z*: 1504 $[M]^+$. UV–vis λ_{max} (nm) (log ε) in DMF: 309 (5.15), 612 (4.26), 687 (4.68). Anal. Calcd for $C_{80}H_{48}N_8O_{20}Cu$: C, 63.85; H, 3.22; N, 7.45; O, 21.26%. Found: C, 63.73; H, 3.34; N, 7.51; O, 21.32%.

*Synthesis of 1(4),8(11),15(18),22(25)-tetrakis [ethyl 7-oxycoumarin-3-carboxylate] phthalocyaninatonickel(II) (**6**)*

The compound was soluble in DMF, DMSO and DMA. Yield: 0.019 (18%). Mp >300°C. FT-IR (KBr) ν_{max} (cm^{-1}): 3081–3043 (Ar-H), 2924–2851 (aliphatic CH), 1717 (C═O), 1610–1457 (Ar C═C), 1317–1260 (Ar-O═C), 1121, 1043, 995, 800, 746. UV–vis λ_{max} (nm) (log ε) in DMF: 293 (4.88), 604 (4.13), 680 (4.51). Anal. Calcd for $C_{80}H_{48}N_8O_{20}Ni$: C, 64.06; H, 3.23; N, 7.47; O, 21.33%. Found: C, 64.23; H, 3.34; N, 7.61; O, 21.38%.

Electrochemical and in situ *spectroelectrochemical measurements*

The cyclic and differential pulse voltammetry (DPV) measurements were carried out with a Gamry Reference 600 Model potentiostat/galvanostat controlled by an external PC and utilising a three-electrode configuration at 25°C. The working electrode was a Pt plate with a surface area of 0.10 cm^2. The surface of the working electrode was polished with H_2O suspension of Al_2O_3 before each run. A Pt spiral wire having a large surface area served as the counter electrode. A saturated calomel electrode (SCE) was employed as the reference electrode and separated from the bulk of the solution by a salt bridge. Electrochemical grade tetrabutylammonium perchlorate (TBAP) in extra pure DMSO was employed as the supporting electrolyte at a concentration of 0.10 mol dm^{-3}. Therefore, the salt bridge used for the reference electrode was filled with the same electrolyte solution. High purity N_2 was used for deoxygenating the solution at least 20 min prior to each run and to maintain a nitrogen blanket during the measurements. *In situ* spectroelectrochemical measurements were carried out by an Agilent Model 8453 diode array spectrophotometer equipped with the potentiostat/galvanostat and utilising an optically transparent thin layer (OTTLE) cell with a three-electrode configuration at 25°C. The working electrode was transparent Pt gauze. A Pt wire counter electrode and an SCE reference electrode separated from the bulk of the solution by a salt bridge were used.

Results and discussion

Synthesis and characterisation

The ligand, ethyl 7-(2,3-dicyanophenoxy)coumarin-3-carboxylate (**1**), was prepared by a base-catalysed nucleophilic aromatic nitro displacement reaction between 1,2-dicyano-3-nitrobenzene and ethyl 7-hydroxycoumarin-3-carboxylate (**2**) in the presence of K_2CO_3 in dry DMF under N_2 atmosphere at 50–60°C in a Schlenk system for 1 day. The crude product was purified by silica gel column chromatography using $CHCl_3$ as the eluent, and the yield was 58%. The IR spectrum of **1** exhibits the intense absorption band at 2232 cm^{-1} corresponding to the —C≡N stretching, and characteristic frequencies at 3051 (Ar-H), 1737 (lactone —C═O), 1571 (α,β-unsaturated —C═C— for lactone ring) and 1249 cm^{-1} (Ar-O-Ar). Alkyl groups (—CH_2—CH_3) gave intense absorptions at 2939–2918 cm^{-1}. Comparison

of the IR spectral data of coumarin **2** and **1** clearly indicates the formation of **1** by the disappearance of the O–H bands of ethyl 7-hydroxycoumarin-3-carboxylate (**2**) at 3420 cm^{-1} and by the appearance of new absorption at 2232 cm^{-1} for nitrile groups. In addition, in the ^{1}H NMR spectrum of **1**, disappearance of the resonance belonging to the phenolic O–H group at 11.3 ppm confirmed the existence of the expected compound **1**. The ^{1}H NMR spectrum of **1** also indicates the aromatic protons at around 7.27–8.04 ppm as multiplets and the signal of the proton of coumarin **1** at position 4 at 8.81 ppm as a singlet and the CH_3–CH_2 protons in the ethoxyl group at the range of 4.30–1.32 ppm as triplet and quartet. In addition to these results, elemental analyses and mass spectra confirmed the proposed structure.

The novel MPcs containing four ethyl 7-oxycoumarin-3-carboxylate moieties (**3**–**6**) were obtained from the reaction of the dicyano derivative (**1**) and the corresponding metal salts [$Zn(OAc)_2{\cdot}2H_2O$, $Co(OAc)_2{\cdot}4H_2O$, Cu(OAc), $Ni(OAc)_2{\cdot}4H_2O$] in 2-chloronaphthalene at 170°C in a sealed glass tube, followed by purification with various solvents (acetone, acetonitrile, ethanol, methanol and diethyl ether), resulting in the corresponding tetra coumarin-substituted MPcs (**3**–**6**) with 18–36% yields (Scheme 1). The spectroscopic characterisation of the newly synthesised ligand **1** and Pcs (**3**–**6**, **3a** and **3b**) included FT-IR, UV–vis, MALDI-TOF and ^{1}H NMR investigations. The results were in accordance with the proposed structures. The results of elemental analyses for carbon, hydrogen, nitrogen and gravimetric methods for metals were consistent with the proposed structure.

The newly synthesised bluish-green MPc products (**3**–**6**) gave a clear solution in DMSO, DMF and DMA due to the polar ethyl carboxylate moieties at the 3-position of all coumarins at the periphery of the Pc core but they were insoluble in water. The hydrochloric acid-catalysed hydrolysis of coumarino-ZnPc (**3**) in DMF at 120°C furnished the corresponding product **3a** with four carboxylic acid groups at the 3-position of all peripheral coumarin moieties with good yield (72%). This compound was slightly soluble in warm water. The existence of the carboxylic group on the coumarin lactone ring was confirmed by the IR spectrum [3374–3141 cm^{-1} (carboxyl OH), 1714 cm^{-1} (lactone —C═O)].

In the ^{1}H NMR spectra of **3a**, the carboxy proton was not observed due to its exchange with the solvent. The coumarin substituents with ethyl carboxylate at the periphery of the Pcs bring out numerous possibilities for binding with different nucleophiles. Treatment of compound **3** with ethyl nipecotate nucleophile afforded the corresponding ethyl 3-carboxynipeconate derivative (**3b**). Cyclotetramerisation of the dinitrile **1** to the MPcs (**3**–**6**) was also confirmed by the disappearance of the sharp C≡N vibration at 2330 cm^{-1}. This is an evidence for the IR-spectra of MPcs (**3**–**6**). All were very similar and showed absorption peaks at 1118–1120, 1092–1093, 1069–1070, 945–950, 870–873 and 752–756 cm^{-1}, which may be assigned to the Pc skeletal vibration. The ester stretching bands and the α,β-unsaturated —C═C— (lactone ring) bands in the FTIR spectra of all coumarino-Pcs (**3**–**6**, **3a** and **3b**) at *ca.* 1738 and 1640 cm^{-1} are evidences for the formation of coumarino-Pcs.

The mass spectra of **3**–**6** confirmed the proposed structures. The mass spectral studies by the MALDI-TOF technique on the newly synthesised compounds were identified at *m/z*: 1507.61 $[M + H]^+$ for **3**, *m/z*: 1501.21 $[M + H]^+$ for **4**, *m/z*: 1503 $[M]^+$ for **5**, *m/z*: 1498 $[M]^+$ for **6**. Values of the molecular ions show good agreement with the calculated values of all MPcs (**3**–**6**) in the presence of α-cyano-4-hydroxycinnamic acid (20 mg/ml in THF) as a matrix (Figure 1, compound **3** as an example).

Figure 2 shows UV–vis spectra of Pc compounds **3**–**6** in DMSO. They displayed characteristic Q band absorptions between 680 and 688 nm (**3** at 688 nm, **4** at 689 nm, **5** at 687 nm and **6** at 680 nm), due to electronic transitions from π-HOMO to π*-LUMO energy levels. These complexes also showed typical B band absorptions between 293 and 317 nm, because of electronic transitions from deeper π-HOMO to π*-LUMO levels. It appears that the B band absorptions of the complexes coincide with the characteristic absorption signal of the coumarin moiety, since it is usually observed between 310 and 346 nm in the near UV region (*4*, *22*). As shown in Figure 2, CoPc (**4**) and CuPc (**5**) showed no evidence of aggregation. Rather, each complex showed a sharp Q band absorption, corresponding only to monomeric forms as well as a vibrational satellite at the blue side of Q band absorption. The aggregation of Pc molecules results mainly from the π–π* interactions between the π electron clouds of adjacent Pc macrocycles (*23*). Some functional groups in Pc molecules enable the formation of aggregation, which results from additional specific interactions such as hydrogen bonding in Pcs containing carboxylic groups (*24*), ester (*4*) or alkylamide (*25*). The coumarins can also build H-type aggregations at carboxyl groups. On the other hand, the lactone carbonyl of coumarins can coordinate metal cations such as Cu^{2+},

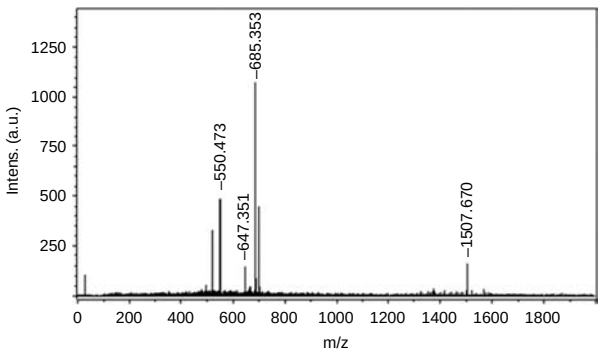

Figure 1. Mass spectrum of **3**.

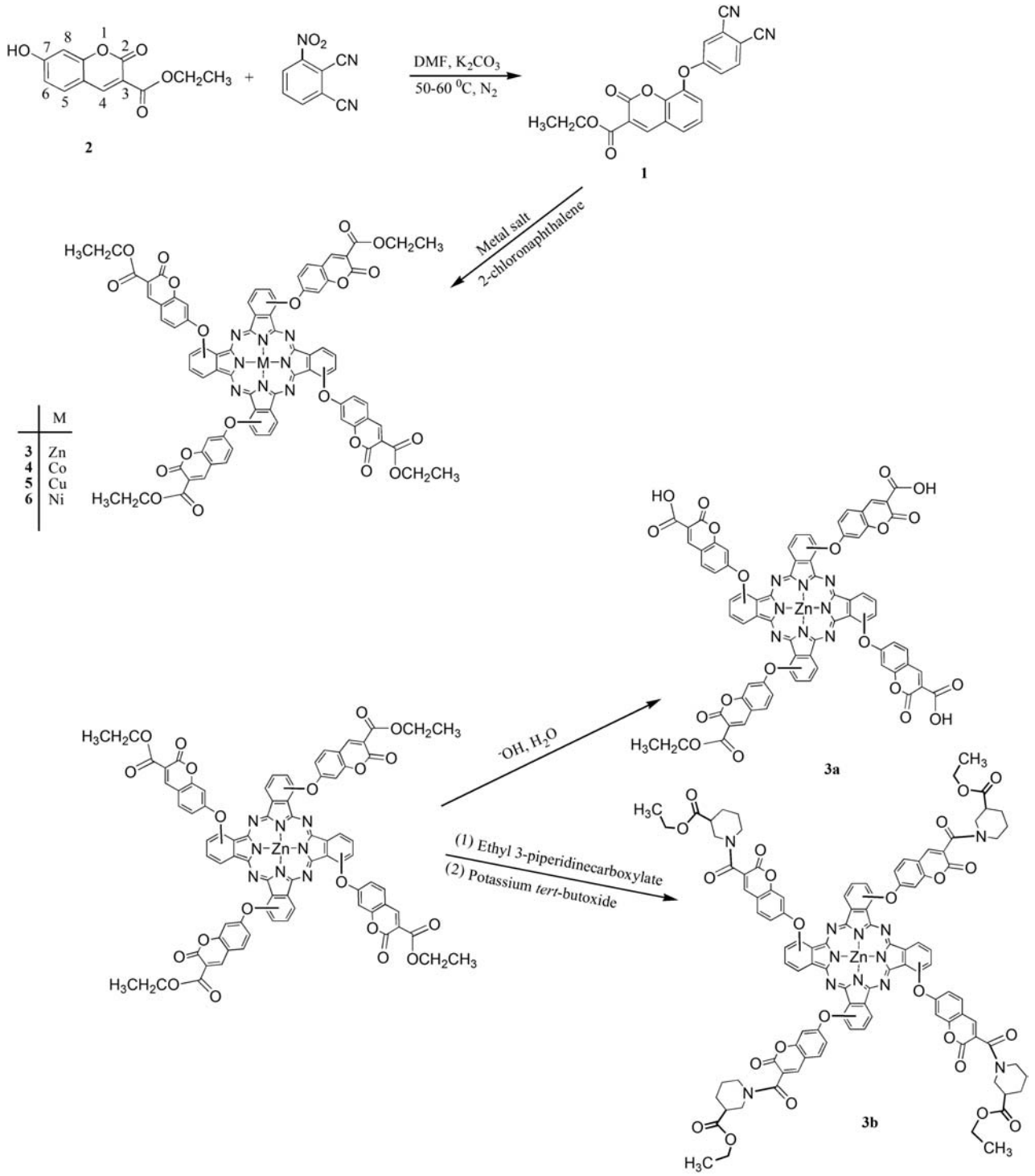

Scheme 1. Synthetic route to ethyl 7-(2,3-dicyanophenoxy)coumarin-3-carboxylate (**1**) and MPcs (**3**–**6**, **3a** and **3b**).

Mn^{2+}, Ni^{2+}, Co^{2+} (*26*). The absence of aggregated species in solutions of **3** and **4**–**6** in DMF may be attributed to the non-peripheral nature of α-substituted coumarin moieties. It has been well established that non-aggregated Pcs are extremely important for their various applications (*27*–*31*). The comparison of the UV–vis spectrum of **3** in Figure 2 with those monitored at different concentrations of **3a** in Figure 3 suggests that the replacement of ethyl groups in **3** with hydrogen atoms gives rise to a very small effect on its electronic absorption spectrum, as a few nanometres blue shift in characteristic absorptions. As expected, the solution of **3a** in DMF also includes only

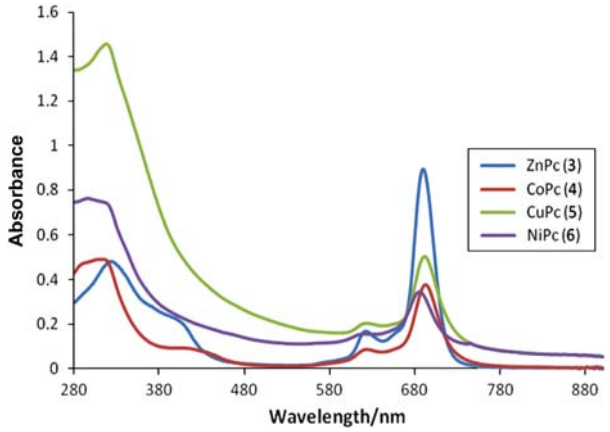

Figure 2. Absorption spectra of **3**–**6** in DMF.

monomeric species, as evidenced from its sharp Q band absorptions in UV–vis spectra monitored at different concentrations. On the other hand, the replacement of ethylcarboxylate groups in **3** with ethyl 3-piperidinecarboxylate moieties strongly affects its UV–vis spectrum, especially in terms of aggregation behaviour. As shown in Figure 4, the solution of **3b** in DMF involves aggregated species, as evidenced from the broadened Q band absorption and the broad shoulder at its blue side. The broad shoulder at the blue side of the Q band absorption provides strong evidence for H-type aggregation. Ethyl 3-piperidinecarboxylate moieties in **3b** probably decrease the non-planarity and, thus, increase the co-planar association between the molecules.

Fluorescence emission spectra for Pcs **3** and **4** in DMF are shown in Figure 5. The ZnPc (**3**) shows fluorescence behaviour with an intensive emission peak at 708 nm (Figure 5(A)). On the other hand, the emission peak of CoPc (**4**) at 708 nm is very weak. As shown in Figure 5(B), the excitation spectrum of **3** is similar to its absorption spectra, and is the mirror image of the fluorescence spectra (*17*). The observed Stokes shifts are typical for Pc complexes (Table 1).

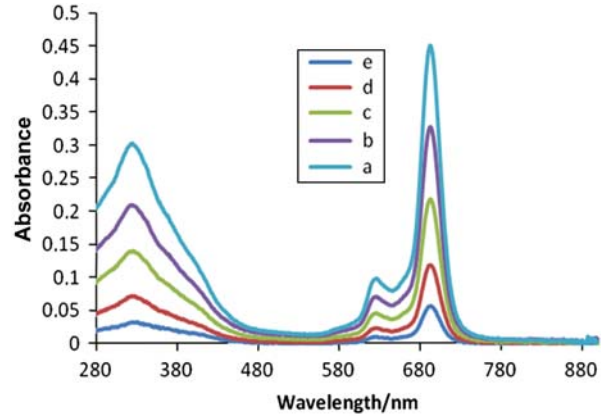

Figure 3. Absorption spectra of **3a** at different concentrations within the range of $1.0 \times 10^{-6} - 8.0 \times 10^{-6}$ mol l^{-1} in DMF.

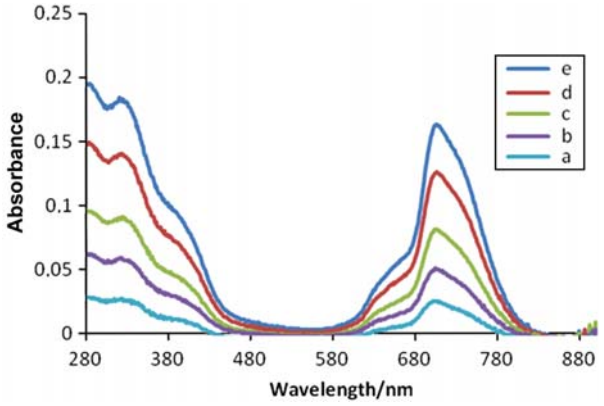

Figure 4. Absorption spectra of **3b** at different concentrations within the range of $1.0 \times 10^{-6} - 8.0 \times 10^{-6}$ mol l^{-1} in DMF.

Electrochemistry and in situ *spectroelectrochemistry*

The electrochemical behaviour of α-tetra 7-oxycoumarin-3-carboxylate-substituted Pcs **3**–**6** was investigated by cyclic voltammetry and DPV in DMSO involving TBAP as the supporting electrolyte. The voltammetric data of **3**–**6**,

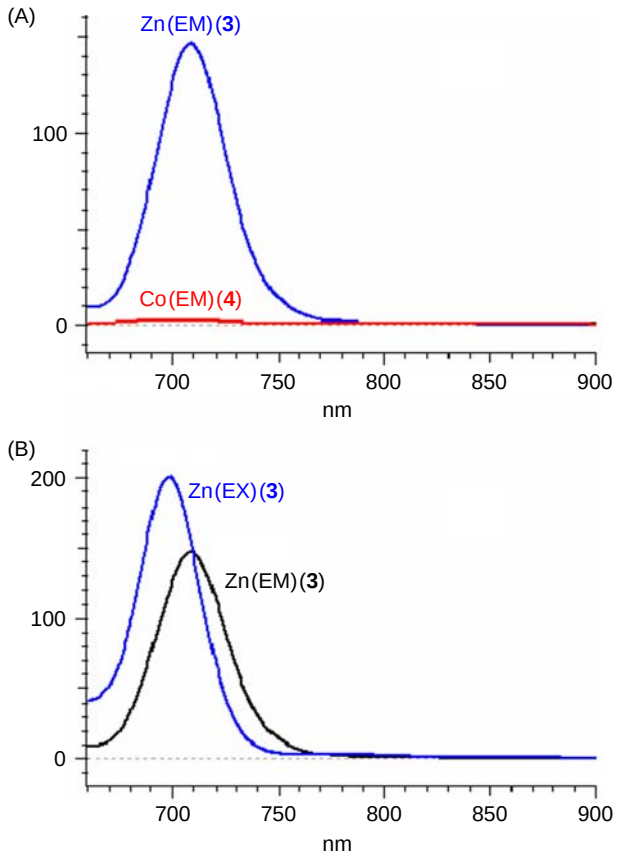

Figure 5. (A) Fluorescence emission spectra of **3** and **4** in DMF (excitation wavelength = 698 nm for **3**; 702 nm for **4**). (B) Fluorescence emission and excitation spectra of **3** in DMF (excitation wavelength = 698 nm).

Table 1. Absorption, excitation and emission spectral data for metal phthalocyanines **3** and **4** in DMF.

Compound	Q band, λ_{max} (nm)	$\log \varepsilon$	Excitation, λ_{ex} (nm)	Emission, λ_{em} (nm)	Stokes shift Δ_{Stokes} (nm)
3	688	4.69	699	709	19
4	689	4.56	702	700	11

including the half-wave potential value vs. SCE ($E_{1/2}$), anodic-to-cathodic peak potential separation (ΔE_p) and the difference between the first oxidation and reduction potential ($\Delta E_{1/2}$) are summarised in Table 2. The number of electrons transferred is unity for all redox processes. However, in monophthalocyanines, multi-electron processes occurring in one step are not common (*32*). ΔE_p values ranged from 60 to 120 mV, thus suggesting reversible to quasi-reversible behaviour. These processes are usually attributed to successive removal of electrons from, or addition of electrons to, the Pc molecules (*32*). The peak currents for the redox processes of the complexes were usually found to be directly proportional to the square root of the scan rate, suggesting their diffusion-controlled nature. From well-defined redox behaviour of monophthalocyanines, all redox couples of **3**, **5** and **6** are attributed to Pc ring-based processes while complex **4** also displays metal-based processes. For this reason, *in situ* spectroelectrochemistry of **4** was only examined to identify its possible metal-based redox processes. Figure 6 shows typical cyclic and differential pulse voltammograms of 5.00×10^{-4} mol dm^{-3} **3** on platinum in DMSO/TBAP.

As shown in Table 2, redox behaviours of **5** and **6** are similar to each other with some differences between their $\Delta E_{1/2}$ values which can be attributed to the differences between the polarising powers of the metal centres. The reduction and oxidation potentials of these complexes are less negative and less positive, respectively, than those of their unsubstituted homologues (*32*). Thus, the half-wave potential differences between the first oxidation and reduction couples, $\Delta E_{1/2}$, of **5** and **6** are also relatively low, as compared to those of their unsubstituted homologues. $\Delta E_{1/2}$ values of these complexes are closely related to their HOMO–LUMO gaps. The values within the range of 1.5–1.7 V were reported for unsubstituted and β-substituted MPcs (*32*). The decrease in the HOMO–LUMO gaps of **5** and **6** in relation to their unsubstituted and β-substituted homologues can be attributed to destabilisation of HOMO and stabilisation of LUMO energy level by electron-rich carboxylated oxycoumarin substituents at non-peripheral positions, as a result of linear combinations of the atomic orbitals. It appears that substitution at the non-peripheral position results in more enhancement of electron density compared to peripheral substitution, resulting in ease of oxidation. However, the half-wave potential for the oxidation couple of **3** is considerably more positive than those of **5** and **6**. As shown in Figure 6, it displays one oxidation (O1) and three reduction (R1–R3) couples. The cyclic voltammetry signal of the oxidation couple is ill-defined due to its placement at the end of the electrolyte-limited positive potential range. However, DPV enabled us to detect this reversible couple. The polarising effect of alpha substituents for this complex appears to be very limited compared to **5** and **6**. This may be due to the presence of species, axially coordinated to the metal centre in the case of **3**.

Figure 7 shows the cyclic and differential pulse voltammograms of **4** (CoPc). It undergoes one oxidation (O1) and three reductions (R1, R2 and R3). Although the last

Table 2. Voltammetric data of α-tetra 7-oxycoumarin-3-carboxylate-substituted MPcs **3**–**6** on Pt in DMSO/TBAP.

Complex	Ring oxidation	M^{II}/M^{III}	M^{II}/M^{I}	Ring reductions			[a]$\Delta E_{1/2}$ (V)
3 (ZnPc)							
[b]$E_{1/2}$ (V)	0.78			−0.69	−0.98	−1.22	1.47
[c]ΔE_p (V)				0.100	0.060	0.060	
4 (CoPc)							
[b]$E_{1/2}$ (V)		0.51	−0.23	−1.15	−1.44		0.74
[c]ΔE_p (V)		0.080	0.120	0.120	0.080		
5 (CuPc)							
[b]$E_{1/2}$ (V)	0.34			−0.62	−0.99		0.96
[c]ΔE_p (V)	0.120			0.100	0.120		
6 (NiPc)							
[b]$E_{1/2}$ (V)	0.41			−0.51	−0.94	−1.41	0.92
[c]ΔE_p (V)	0.120			0.060	0.120	0.100	

[a] $\Delta E_{1/2} = E_{1/2}$ (first oxidation) − $E_{1/2}$ (first reduction).
[b] $E_{1/2} = (E_{pa} + E_{pc})/2$ at 0.050 V s^{-1}. The potentials refer to SCE.
[c] $\Delta E_p = E_{pa} + E_{pc}$ at 0.050 V s^{-1}.

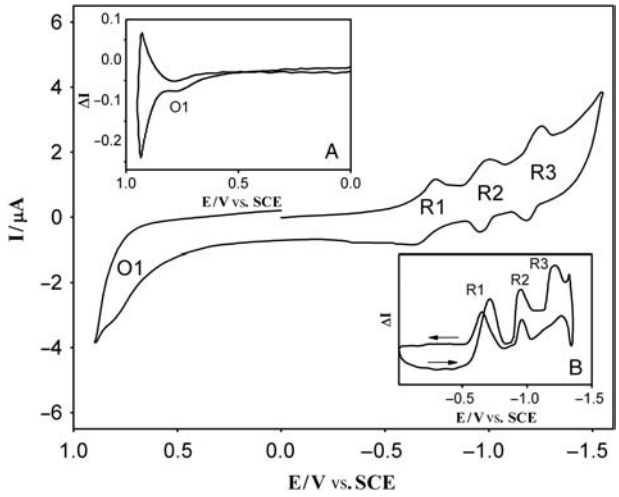

Figure 6. Cyclic and cyclic differential pulse (insets A and B) voltammograms of 5.0×10^{-4} mol dm^{-3} **3** in TBAP/DMSO at 0.050 V s^{-1} (DPV parameters: pulse time, 50 ms; pulse size, 100 mV; step size, 5 mV; sample period, 100 ms).

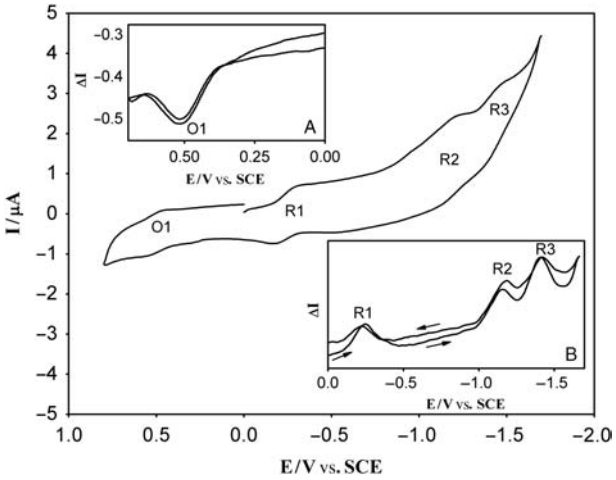

Figure 7. Cyclic and cyclic differential pulse (insets A and B) voltammograms of 5.0×10^{-4} mol dm^{-3} **4** in TBAP/DMSO at 0.050 V s^{-1} (DPV parameters: pulse time, 50 ms; pulse size, 100 mV; step size, 5 mV; sample period, 100 ms).

two reduction couples of its cyclic voltammogram are ill-defined, DPV enabled us to define the potentials and reversibility of all its redox processes. Co(II) centre in **4** may have accessible d orbital levels lying between the HOMO and LUMO gap of the Pc ligand, depending on whether there are any available coordinating species that would stabilise it, and thus, can be oxidised and reduced before the ring-based redox processes. For this reason, *in situ* spectroelectrochemical measurements were also carried out to assign the redox processes of **4**, especially the first reduction and the first oxidation. Figure 8(A) shows the spectral changes observed across the first reduction of **4**. With the progress of electrolysis, the Q band absorption decreases with red shift from 681 to 686 nm. This spectral change is accompanied by formation of a new band at 474 nm in the region between the Q and Soret bands. Two isosbestic points were detected at 398 and 568 nm. These are similar to the changes observed to date for many CoPc derivatives when Co(II) was reduced to Co(I), and the band developed between the Q and Soret bands has been assigned to the metal-to-ligand charge transfer from cobalt to ligand b_{1u} and b_{2u} orbitals under D_{4h} symmetry (*33–36*). Thus, it is very clear that the first reduction occurs at the cobalt centre. The subsequent second and third reductions occur on the Pc ring in comparison with the literature (*32*), and correspond to $[Co(I)Pc(-2)]^{-}/[Co(I)Pc(-3)]^{2-}$ and $[Co(I)Pc(-3)]^{2-}/[Co(I)Pc(-4)]^{3-}$, respectively. Figure 8(B) displays spectral changes during the first oxidation process. The Q band at 681 nm increases in intensity with red shift to 690 nm. The increase of the Q band with red shift is typical of a metal-based oxidation in CoPc complexes, and thus indicates clearly that the O1 couple of **4** corresponds to the $Co(II)Pc(-2)/[Co(III)Pc(-2)]^{+}$ process (*37–39*). The occurrence of the first reduction and the first

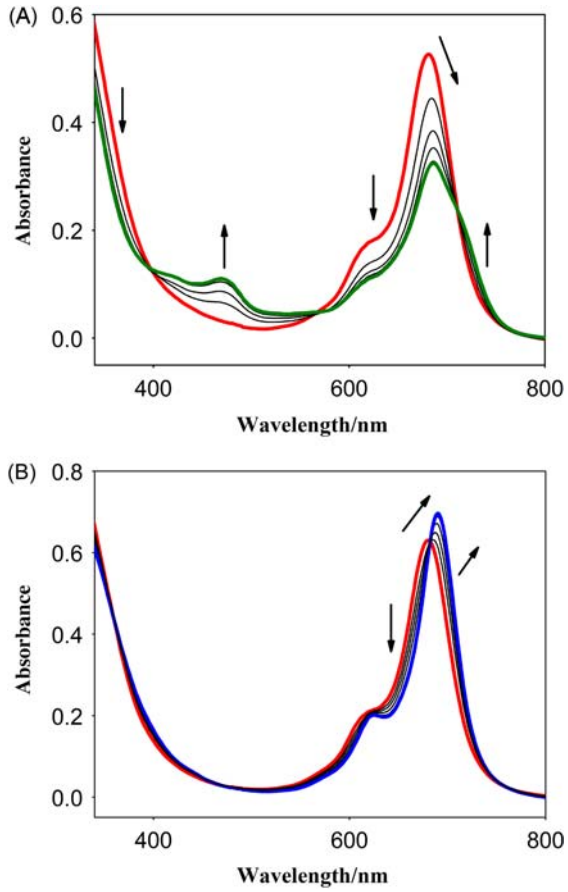

Figure 8. *In situ* UV–vis spectral changes during the first reduction and oxidation processes of **4** at (A) −0.30 V and (B) 0.60 V vs. SCE, respectively, in TBAP/DMSO.

oxidation processes on the metal centre, evidenced from spectroelectrochemical measurements, confirms the idea that complex **4** has accessible d orbital levels lying between the HOMO and LUMO gap of the Pc species. It is noteworthy that the half-wave redox potential for the first reduction of α-substituted **4** (− 0.23 V vs. SCE) is less negative than that of a previously reported (*22*) β-substituted similar one (− 0.47 V vs. SCE). The substitution at α positions shifts the first oxidation potential also in the positive direction (30 mV), as compared to the relevant potential of β-substituted similar CoPc (0.48 V vs. SCE). These shifts can be attributed to the effect of non-peripheral α substitution on the energy levels of metal-based orbitals, playing the role in the first reduction and first oxidation processes.

Conclusions

In conclusion, we have achieved the synthesis and characterisation of novel coumarino-MPcs (ZnPc (**3**), CoPc (**4**), CuPc (**5**) and NiPc (**6**)) by cyclotetramerisation of ethyl 7-(2,3-dicyanophenoxy)coumarin-3-carboxylate (**1**) with relevant metal salts. These complexes are soluble in polar organo solvents. The acid hydrolysis of ester groups at 3-positions of coumarin moieties in **3** gave their derivatives bearing carboxylic acid groups and slightly soluble in water. The product obtained by the reaction of **3** with ethyl nipecotate, **3b**, also demonstrated the derivatisability of **3**. It was concluded from the electrochemical measurements that tetra-alpha substitution of Cu(II) and Ni(II) Pcs by 7-oxy-coumarin-3-carboxylate groups at non-peripheral positions of the Pc ring shifts the first reduction and, especially, the first oxidation potential towards less negative and less positive potentials, respectively, as a result of the linear combination of atomic orbitals, compared to their unsubstituted and beta-substituted analogues. Thus, the HOMO–LUMO gaps of **5** and **6** are considerably narrow, in comparison with their unsubstituted and beta-substituted analogues.

Acknowledgement

We are thankful to the Scientific and Research Council of Turkey (TÜBİTAK) (107T347 and 108T623).

References

(1) Leznoff, C.C.; Lever, A.B.P. In *Phthalocyanines: Properties and Applications*; Leznoff, C.C., Lever, A.B.P., Eds.; VCH: Weinheim, 1989–1996; Vols. 1–4.
(2) Moser, F.H.; Thomas, A.L. In *The Phthalocyanines Properties*; Thomas, A.L., Ed.; CRC: Boca Raton, FL, 1983; p 79.
(3) Hanack, M.; Heckmann, H.; Polley, R. In *Methods of Organic Chemistry (Houben-Weyl)*; 4th ed.; Schaumann, E., Ed.; Georg Thieme Verlag: Stuttgart, 1997; Vol. E9d, p 717.
(4) Çamur, M.; Özkaya, A.R.; Bulut, M. *Polyhedron* **2007**, *262*, 2638–2646.
(5) Esenpınar, A.A.; Bulut, M. *Dyes Pigments* **2008**, *76*, 249–255.
(6) Murray, R.D.H.; Mendez, J.; Brown, S.A. *The Natural Coumarins: Occurrence Chemistry and Biochemistry*; Wiley & Sons: New York, 1982.
(7) Tiew, P.; Ioset, J.R.; Kokpal, U.; Chavasir, W.; Hostettmam, K. *Phytother. Res.* **2003**, *17*, 190–193.
(8) Jurd, L.K.; Mihara, K. *Phytochemistry* **1971**, *10*, 2965–2970.
(9) Sardari, S.; Mori, Y.; Horita, K.; Micetich, R.G.; Nishibe, S.; Daneshtalab, M. *Bioorg. Med. Chem.* **1999**, *7*, 1933–1940.
(10) Mazzei, M.; Dondero, R.; Sottotattari, E.; Melloni, E.; Minafra, R. Eur *J. Med. Chem.* **2001**, *36*, 851–861.
(11) Kasinadhuni, V.R.R.; Rajashekbar, G.; Rajogopalan, R.; Sharma, V.M.; Krishna, C.V.; Sairam, P.; Prasad, G.S.; Sadhukhan, S.; Rao, G.G. *Fitoterapia* **1999**, *70*, 93–95.
(12) Nath, M.; Jairath, R.; Eng, G.; Song, X.; Kumar, A. *J. Organomet. Chem.* **2005**, *690*, 134–144.
(13) Yu, D.; Suzuki, M.; Xie, L.; Morris-Natschke, S.L.; Lee, K.H. *Med. Res. Rev.* **2003**, *23*, 322–345.
(14) O'Kennedy, R.; Thornes, R.D. *Coumarins: Biology, Applications and Mode of Action*; Wiley & Sons: Chichester, 1997.
(15) Bamfield, P. *Chromic Phenomena: Technological Application of Colour Chemistry*; The Royal Society of Chemistry: Cambridge, 2001.
(16) Çamur, M.; Bulut, M. *Dyes Pigments* **2008**, *77*, 165–170.
(17) George, R.D.; Snow, A.W. *Heterocyclic Chem.* **1995**, *32*, 495–498.
(18) Petty, F.; Coffmann, J.A. *Neuropharmacology* **1984**, *23*, 859–860.
(19) Ross, S.M.; Craig, C.R. *J. Neurochem.* **1981**, *36*, 1006–1011.
(20) Esenpınar, A.A.; Özkaya, A.R.; Bulut, M. *Polyhedron* **2009**, *28*, 33–42.
(21) Kenney, M.E.; Oleinick, N.L.; Rihter, B.D.; Li, Y.S. Phthalocyanine photosensitizers for photodynamic therapy and methods for their use. US Patent 5484778, Jan 16, 1996.
(22) Alemdar, A.; Özkaya, A.R.; Bulut, M. *Polyhedron* **2009**, *28*, 3788–3796.
(23) Suchan, A.; Nackiewicz, J.; Hnatejko, Z.; Waclawek, W.; Lis, S. *Dyes Pigments* **2009**, *80*, 239–244.
(24) Fujiki, M.; Tabei, H.; Kurihara, T.J. *J. Phys. Chem.* **1988**, *92*, 1281–1285.
(25) Thati, B.; Noble, A.; Rowan, R.; Creaven, B.S.; Walsh, M.; McCann, M.; Egan, D.; Kovanagh, K. *Toxicol. In Vitro* **2007**, *21*, 801–808.
(26) Creaven, B.S.; Egan, D.A.; Karcz, D.; Kavanagh, K.; McCann, M.; Mahon, M.; Noble, A.; Thati, B.; Walsh, M. *Int. J. Biochem. Cell Biol.* **2007**, *101*, 1108–1119.
(27) Snow, A.W. In *The Porphyrin Handbook*; Kadish, K.M., Smith, K.M., Guillard, R., Eds.; Academic: San Diego, CA, 2003; Vol. 17, p 129.
(28) Kasuga, K.; Hayashi, H.; Handa, M. *Chem. Lett.* **1991**, 1877–1880.
(29) Sharman, W.M.; Kudrevich, S.V.; Van Lier, J.E. *Tetrahedron Lett.* **1996**, *37*, 5831–5834.
(30) George, R.D.; Snow, A.W.; Shirk, J.S.; Barger, W.R. *J. Porphyr. Phthalocya.* **1998**, *2*, 1–7.
(31) Lang, K.; Kubat, P.; Mosinger, J.; Wagnerova, D.M.J. *J. Photochem. Photobiol. A.* **1998**, *119*, 47–52.
(32) Lever, A.B.P.; Milaeva, E.R.; Speier, G. In *Phthalocyanines: Properties and Applications*; Leznoff, C.C., Lever, A.B.P., Eds.; VCH: New York, 1993; Vol. 3, pp 1–69.
(33) Stillman, M.J.; Thomson, A.J. *J. Chem. Soc. Faraday Trans. 2* **1974**, *70*, 790–804.

(34) Hesse, K.; Schlettwein, D. *J. Electroanal. Chem.* **1999**, *476*, 148–158.
(35) Özer, M.; Altındal, A.; Özkaya, A.R.; Bulut, M.; Bekaroğlu, Ö. *Polyhedron* **2006**, *25*, 3593–3602.
(36) Koca, A.; Özkaya, A.R.; Arslanoğlu, Y.; Hamuryudan, E. *Electrochim. Acta* **2007**, *52*, 3216–3221.
(37) Koca, A.; Özkaya, A.R.; Selçukoğlu, M.; Hamuryudan, E. *Electrochim. Acta* **2007**, *52*, 2683–2690.
(38) Jin, Z.; Nolan, K.; McArthur, C.R.; Lever, A.B.P.; Leznoff, C.C. *J. Organomet. Chem.* **1994**, *468*, 205–212.
(39) Tse, Y.H.; Goel, A.; Hu, M.; Leznoff, C.C.; Van Lier, J.E.; Lever, A.B.P. *Can. J. Chem.* **1993**, *71*, 742–753.